DYNAMICS OF NONLINEAR BAROCLINIC EKMAN BOUNDARY LAYER

Liu Qinyu (刘秦玉) and *Qin Zenghao* (秦曾灏)*

Shandong College of Oceanology, Qingdao

Received August 23, 1985

ABSTRACT

By the geostrophic momentum approximation, the wind structure and vertical motion within the nonlinear baroclinic Ekman layer matching with the surface layer are determined. A comparison of the Ekman solution with the classical one is made. It is demonstrated that the contributions of baroclinity, stratification and nonlinear effects to the wind profile within the layer are all of definite importance.

I. INTRODUCTION

The wind distribution within the atmospheric boundary layer, which is the passage from the free atmosphere to the earth's surface, has its prime importance in affecting both the motion in the free atmosphere and the transport of the physical properties such as mass, momentum, heat, water vapour and suspended particles, so that the accurate determination of the wind distribution with height within the layer is closely related to environmental pollution, offshore oil exploitation, marine transportation, and other activities at sea.

In recent years, a great many of research papers to improve the classical Ekman solution in different respects have appeared and have yielded many significant results.

By introduction of the geostrophic momentum approximation, Wu and others[1-3] pointed out that the correction of the nonlinear advection to both the wind profile in the Ekman boundary layer and the vertical current at the top of the layer is not negligibly small. However, they ignored the effects of baroclinity and stratification on the distribution of wind with height. In this paper, those factors together with the nonlinear advection effect are all to be taken into account to investigate the dynamic characteristics of the Ekman boundary layer by a two-layer planetary boundary layer (PBL) model. Some useful conclusions are reached.

II. BASIC EQUATIONS AND BOUNDARY CONDITIONS

The PBL is assumed to be subdivided into the surface layer ($z_0 \leqslant z \leqslant h$) and the overlaying Ekman layer ($h \leqslant z \leqslant H$). Assuming the constant eddy viscosity coefficient K against height and neglecting the horizontal momentum transfer by eddy within the Ekman boundary layer, we obtain the governing equations as follows:

*Present affiliation: Shanghai Institute of Typhoon, Shanghai.

$$\frac{\partial u}{\partial t}+u\frac{\partial u}{\partial x}+v\frac{\partial u}{\partial y}-f(v-v_g)=K\frac{\partial^2 u}{\partial z^2},$$

$$\frac{\partial v}{\partial t}+u\frac{\partial v}{\partial x}+v\frac{\partial v}{\partial y}+f(u-u_g)=K\frac{\partial^2 v}{\partial z^2}, \tag{1}$$

$$\frac{\partial u}{\partial x}+\frac{\partial v}{\partial y}+\frac{\partial w}{\partial z}=0,$$

where (u, v, w) are the velocity components along the coordinate axes (x, y, z), and (u_g, v_g) are two horizontal components of geostrophic wind. Other symbols have the same meanings as those conventionally used in atmospheric sciences.

The governing equation in the surface layer has the form:

$$\frac{\partial v}{\partial z}=\frac{u_*}{kz}\phi\left(\frac{z}{L}\right), \tag{2}$$

where $U=\sqrt{u^2+v^2}$, $L=-\dfrac{u_*^3 C_p\rho\bar{\theta}}{kgH}$ is Monin–Obukhov length; k Von kaman constant $(k=0.4)$; $u_*=(\tau/\rho)^{1/2}$ the friction velocity; $\theta_*=-\dfrac{H_h}{\rho C_p u_*}$ the scaling temperature, with H_h being the eddy heat flux and ϕ the universal function describing stratification. The corresponding boundary conditions are assumed as follows.

(1) The top boundary $(z=H)$:

$$u=u_H, \qquad v=v_H, \tag{3}$$

where u_H and v_H satisfy the following equations:

$$\frac{\partial u}{\partial t}+u\frac{\partial u}{\partial x}+v\frac{\partial u}{\partial y}-f(v-v_g)=0,$$

$$\frac{\partial v}{\partial t}+u\frac{\partial v}{\partial x}+v\frac{\partial v}{\partial y}+f(u-u_g)=0.$$

(2) The bottom boundary $(z=z_0)$:

$$u=v=0. \tag{4}$$

(3) The inner boundary $(z=h)$:

$$u=u_h, \qquad v=v_h, \qquad K=K_h=\frac{khu_*}{\phi(h/L)}. \tag{5}$$

The inner boundary conditions connect the Ekman layer with the surface layer. Therefore u_h, v_h and K_h on the inner boundary reflect the influences of the stratification and the earth's surface roughness on the wind velocity within the Ekman boundary leyer.

In the surface layer, the solution of Eq. (2) satisfying bottom condition (4) is:

$$U(z)=\frac{u_*}{k}[\ln(z/z_0)-\Psi(z/L)], \qquad (h\geqslant z\geqslant z_0) \tag{6}$$

where $\Psi(z/L)=\int_0^{z/L}\dfrac{1-\phi(\rho')}{\rho'}d\rho'$, and the function ϕ given by Businger et al.[3] on the basis of observations can be expressed as follows

$$\phi(z/L)=(1-15z/L)^{-1/4}, \quad L<0, \quad \text{unstable}$$
$$\phi(z/L)=1+4.7z/L, \quad L>0, \quad \text{stable}$$
$$\phi(z/L)=1. \quad L\to\infty, \quad \text{neutral}$$

Because the inner parameters u_*, θ_*, L, etc. are determined from the specified surface temperature and outer parameters of the atmospheric boundary layer by means of the combination of the solution of the Ekman layer with that of the surface layer, we can determine the u_h, v_h, and K_h at the bottom of the Ekman layer $z=h$.

III. BAROCLINIC EKMAN SOLUTION COMPRISING NONLINEAR ADVECTION TERM

In order to make the solution more applicable, we consider a baroclinic atmosphere, in which (1) the horizontal temperature gradient does not vary with height and (2) the horizontal variability of horizontal temperature gradient is so weak that it can be safely neglected.

To simplify the problem, we adopt the coordinate transformation $\eta=E(z-h)$, where $E=\left(\frac{f}{2K}\right)^{1/2}$, and introduce the geostrophic momentum approximation[1]:

$$\frac{du}{dt}=\frac{du_g}{dt}=\left(\frac{\partial}{\partial t}+u\frac{\partial}{\partial x}+v\frac{\partial}{\partial y}\right)u_g,$$
$$\frac{dv}{dt}=\frac{dv_g}{dt}=\left(\frac{\partial}{\partial t}+u\frac{\partial}{\partial x}+v\frac{\partial}{\partial y}\right)v_g, \tag{7}$$

then the Eq. (1) is transformed to

$$\frac{1}{f}\left(\frac{\partial u_g}{\partial t}+u\frac{\partial u_g}{\partial x}+v\frac{\partial u_g}{\partial y}\right)-(v-v_g)=\frac{1}{2}\frac{\partial^2 u}{\partial\eta^2},$$
$$\frac{1}{f}\left(\frac{\partial v_g}{\partial t}+u\frac{\partial v_g}{\partial x}+v\frac{\partial v_g}{\partial y}\right)+(u-u_g)=\frac{1}{2}\frac{\partial^2 v}{\partial\eta^2}, \tag{8}$$
$$\frac{\partial u}{\partial x}+\frac{\partial v}{\partial y}+\frac{\partial\tilde{w}}{\partial\eta}=0,$$

where $\tilde{w}=(f/2K)^{1/2}w$.

Based on assumption (2) in this section, the first two equations of (8) may be expressed in the following equivalent form:

$$\frac{1}{2}\frac{\partial^2 u}{\partial\eta^2}+a_1u+b_1v=c_1(\eta),$$
$$\frac{1}{2}\frac{\partial^2 v}{\partial\eta^2}+a_2u+b_2v=c_2(\eta), \tag{9}$$

where

$$a_1=-\frac{1}{f}\frac{\partial u_{g0}}{\partial x}, \quad b_1=1-\frac{1}{f}\frac{\partial u_{g0}}{\partial y}, \quad c_1(\eta)=v_g(\eta)+\frac{1}{f}\frac{\partial}{\partial t}[u_g(\eta)],$$
$$a_2=-\left(1+\frac{1}{f}\frac{\partial v_{g0}}{\partial x}\right), \quad b_2=-\frac{1}{f}\frac{\partial v_{g0}}{\partial y}, \quad c_2(\eta)=-u_g(\eta)+\frac{1}{f}\frac{\partial}{\partial t}[v_g(\eta)],$$

and (u_{g0}, v_{g0}) are respectively (x, y) components of the surface geostrophic wind. The boundary conditions subjected to Eq. (9) are:

$$\eta=0, \quad u=u_h, \quad v=v_h, \tag{10}$$

$$\eta\to\infty, \quad u=u_H, \quad v=v_H. \quad (u, v \text{ bounded}) \tag{11}$$

The solution to Eq. (9) satisfying the conditions (10) and (11) gives

$$\begin{aligned} u&=\bar{u}(\eta)+[u_h-\bar{u}(0)]e^{-D\eta}\cos(D\eta)+B_1e^{-D\eta}\sin(D\eta),\\ v&=\bar{v}(\eta)+[v_h-\bar{v}(0)]e^{-D\eta}\cos(D\eta)+B_2e^{-D\eta}\sin(D\eta), \end{aligned} \tag{12}$$

where

$$B_1=[a_1u_h+b_1v_h-c_1(0)]/D^2, \qquad B_2=[a_1u_h+b_1v_h-c_2(0)]/D^2,$$
$$D^4=a_1b_2-a_2b_1,$$
$$\bar{u}(\eta)=[c_1(\eta)b_2-c_2(\eta)b_1]/D^4,$$
$$\bar{v}(\eta)=[a_1c_2(\eta)-a_2c_1(\eta)]/D^4.$$

If the vertical coordinate is returned to the normal z-coordinate, then solution (12) can be reduced to

$$\begin{aligned} u&=\bar{u}(z)+[u_h-\bar{u}(h)]e^{-DE(z-h)}\cos[DE(z-h)]\\ &\quad+B_1e^{-DE(z-h)}\sin[DE(z-h)],\\ v&=\bar{v}(z)+[v_h-\bar{v}(h)e^{-DE(z-h)}\cos[DE(z-h)]\\ &\quad+B_2e^{-DE(z-h)}\sin[DE(z-h)]. \end{aligned} \tag{13}$$

If the terms incorporating local change and nonlinear advection are neglected, then $a_1=0$, $a_2=-1$, $b_1=1$, $b_2=0$, $D=1$, $\bar{u}(z)=u_g(z)$, and $\bar{v}(z)=v_g(z)$. Thus we can obtain the classical Ekman solution

$$\begin{aligned} u&=u_g(z)+[u_h-u_g(h)]e^{-E(z-h)}\cos E(z-h)\\ &\quad+[v_h-v_g(h)]e^{-E(z-h)}\sin E(z-h),\\ v&=v_g(z)+[v_h-v_g(h)]e^{-E(z-h)}\cos E(z-h)\\ &\quad-[u_h-u_g(h)]e^{-E(z-h)}\sin E(z-h). \end{aligned} \tag{14}$$

IV. VERTICAL CURRENTS

With the aid of Eq. (12), we can rewrite the continuity equation as

$$\begin{aligned} \frac{\partial\bar{w}}{\partial\eta}&=-\left[\frac{\partial\bar{u}(\eta)}{\partial x}+\frac{\partial\bar{v}(\eta)}{\partial y}\right]-\left[\left(\frac{\partial u_h}{\partial x}+\frac{\partial v_h}{\partial y}\right)-\left(\frac{\partial\bar{u}(0)}{\partial x}+\frac{\partial\bar{v}(0)}{\partial y}\right)\right]e^{-D\eta}\cos(D\eta)\\ &\quad-\left[\left(u_h-\bar{u}(0)\right)\frac{\partial}{\partial x}+\left(v_h-\bar{v}(0)\right)\frac{\partial}{\partial y}\right]e^{-D\eta}\cos(D\eta)\\ &\quad-\left(\frac{\partial B_1}{\partial x}+\frac{\partial B_2}{\partial y}\right)e^{-D\eta}\sin(D\eta)-\left(B_1\frac{\partial}{\partial x}+B_2\frac{\partial}{\partial y}\right)e^{-D\eta}\sin(D\eta). \end{aligned} \tag{15}$$

Since $\frac{\partial\bar{u}(\eta)}{\partial x}=\frac{\partial\bar{u}(0)}{\partial x}$, $\frac{\partial\bar{v}(\eta)}{\partial y}=\frac{\partial\bar{v}(0)}{\partial y}$ and the functions u_h, v_h, $\frac{\partial\bar{u}}{\partial x}$, $\frac{\partial\bar{v}}{\partial y}$, B_1, B_2 are all independent of the vertical coordinate η, integrating Eq. (15) with respect to η yields

$$\begin{aligned} \bar{w}&=-\left(\frac{\partial\bar{u}}{\partial x}+\frac{\partial\bar{v}}{\partial y}\right)\left(\eta-\frac{1}{2D}\right)-\frac{1}{2D}\left(\frac{\partial u_h}{\partial x}+\frac{\partial v_h}{\partial y}\right)-\frac{1}{2D}\left(\frac{\partial B_1}{\partial x}+\frac{\partial B_2}{\partial y}\right)\\ &\quad-\frac{1}{2}\left\{[u_h-\bar{u}(0)]\frac{\partial}{\partial x}\left(\frac{1}{D}\right)+[v_h-\bar{v}(0)]\frac{\partial}{\partial y}\left(\frac{1}{D}\right)\right\}-\frac{1}{2}\left[B_1\frac{\partial}{\partial x}\left(\frac{1}{D}\right)+B_2\frac{\partial}{\partial y}\left(\frac{1}{D}\right)\right]. \end{aligned} \tag{16}$$

Supposing that the nonlinear advection terms are omitted, hence $\bar{u}=u_g$, $\bar{v}=v_g$, $D\equiv 1$, and that $u_h=v_h=0$, then we obtain

$$\bar{w}=\frac{1}{2}\left(\frac{\partial v_g}{\partial x}-\frac{\partial u_g}{\partial y}\right)=\frac{1}{2}\zeta_g. \tag{17}$$

This is the earlier result derived by Charney and Eliassen[4].

Solution (16) shows that the factors inducing vertical motions at the top of the atmospheric boundary layer are the nonlinear term, stratification and roughness length z_0 as well as the geostrophic vorticity.

V. EXAMPLE

An example will be analysed in this section in order to test the effects of nonlinear advection, baroclinity and stratification on the wind profile and vertical velocity within the PBL.

Assuming an idealized height field $\phi=u_{g0}f_0\left[-y+\frac{1}{M}\sin(Mx)\right]$ on the 1000 hPa isobaric surface, where M is wave number, we have:

$$v_{g0}=u_{g0}\cos(Mx),$$
$$\zeta_{g0}=-Mu_{g0}\sin(Mx).$$

Here, the parameters are assumed to be $u_{g0}=10$ m s^{-1}, $f_0=0.0001$ s^{-1}, $h=50$ m for the inner boundary height and $H=1550$ m for the top boundary height. In addition, the vertical shears of geostrophic wind are taken as $\partial u_g/\partial z=0.005$ s^{-1} or 0.0005 s^{-1} and $\partial v_g/\partial z=0$ s^{-1}.

The earth's surface is chosen to be the sea surface. Two roughness lengths i. e. $z_0=0.00765$ cm and $z_0=0.0019$ cm are adopted. Moreover, u_h and v_h on the inner boundary are calculated with three different stratifications: (a) sea surface temperature (SST) and air temperature (AT) are respectively equal to 0°C and 5°C (stable condition); (b) both SST and AT are equal to 5°C. (neutral condition) ; (c) SST and AT are equal to 10°C and 5°C respectively (unstable condition).

With the geostrophic momentum approximation the hodographs of the wind velocity within the PBL at the geopotential trough $\left[x=\left(\frac{3\pi}{2}+2N\pi\right)/M\right]$ and ridge $[x=(\pi/2+2N\pi)/M]$ under the conditions of $M=2\times10^{-6}$ m^{-1} are shown in Figs. 1a—1i. Figs. 1a—1f and 1g—1i are drawn for the cases of different roughness lengths, stratifications and baroclinities.

It can be seen from Figs. 1a—1i that

(1) based on the geostrophic approximation, the derived solution of wind velocity comprising nonlinear advection effect is greater than the classical Ekman solution at the geopotential ridge; the opposite is true at the geopotential trough;

(2) the stratification not only alters the magnitude of the wind velocity but also influences to some degree the wind distribution in the lower Ekman layer; however, its influence on the wind in the upper Ekman layer is relatively small; and

(3) baroclinity exerts stronger influence on the wind distribution with increasing height; therefore, the neglect of baroclinic effect in discussing the wind distribution in the upper Ekman layer is unsuitable

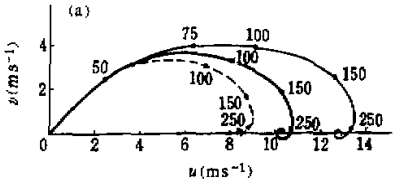

Fig. 1a. Hodograph of the wind under the stable condition within the PBL with z_0=0.0019 cm and $\frac{\partial u_g}{\partial z}$=0.0005 s^{-1}, $\frac{\partial v_g}{\partial z}$=0.

The thick solid line represents the classical Ekman (spiral) solution at ridge and trough lines. The thin solid and dashed lines indicate nonlinear Ekman solution under the geostrophic momentum approximation at ridge and trough lines, respectively. The figures along curves indicate the height of corresponding wind.

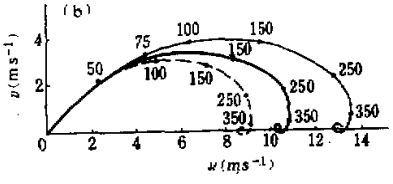

Fig. 1b. Same as Fig. 1a, except for neutral condition.

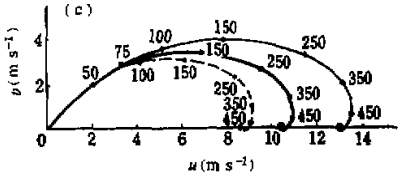

Fig. 1c. Same as Fig. 1a, except for unstable condition.

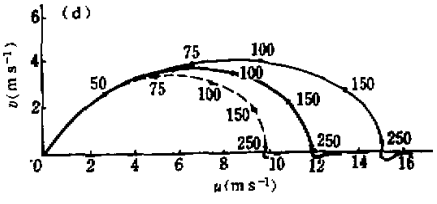

Fig. 1d. Same as Fig. 1a, except for $\partial u_g/\partial z$= 0.005 s^{-1} and stable stratification.

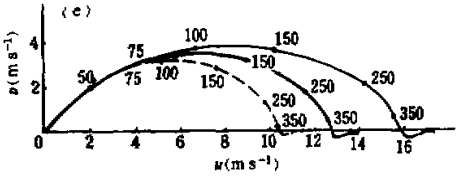

Fig. 1e. Same as Fig. 1d, except for neutral condition.

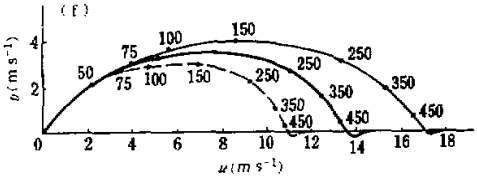

Fig. 1f. Same as Fig. 1d, except for unstable stratification.

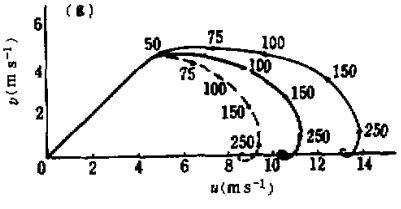

Fig. 1g. Same as Fig. 1a, except for z_0= 0.00765 cm and stable condition.

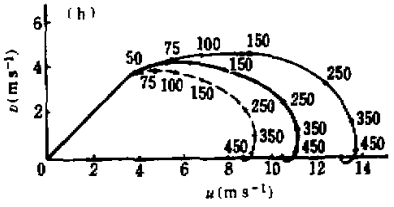

Fig. 1h. Same as Fig. 1g, except for neutral condition.

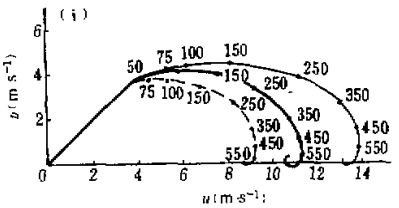

Fig. 1i. Same as Fig. 1g, except for unstable stratification.

Also, we examine the contribution of the nonlinear advection effect to the vertical velocity at the top of the layer with different values of M under the three different stratifications mentioned above. The calculated results are illustrated in Figs. 2a—2c. From these figures, we can draw the following conclusions:

(1) If we take into consideration of the nonlinear advection effect, the absolute value of vertical velocity thus obtained is greater than that from the classical linear Ekman solution at the geopotential ridge. The opposite conclusion is true at the geopotential trough.

(2) The distinction between the vertical velocities with and without consideration of the nonlinear advection becomes remarkable as wave number M increases. This means that the nonlinear advection contributes considerably to the vertical velocity for the synoptic disturbance with shorter waves.

(3) The contribution of stratification to the vertical velocity increases with increasing wave number M. Considering nonlinear advection effect, the influence of the stratification on the vertical velocity becomes remarkable especially at the ridge of the synoptic system with shorter waves.

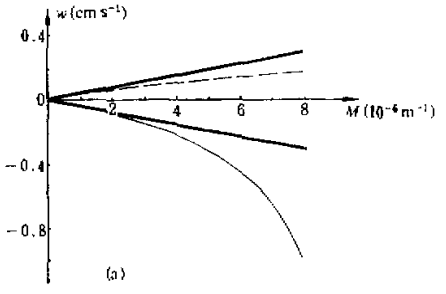

Fig. 2a. Diagram showing the relationship between the vertical velocity and wavenumber of the pressure system under the condition of stable stratification.
The thick solid line indicates the vertical velocity at the ridge and trough lines without consideration of nonlinear effect. The thin solid and dashed lines indicate the vertical velocity at the ridge and trough lines taking account of nonlinear effect, respectively.

VI. CONCLUSIONS

From the foregoing analyses and discussions, we can conclude as follows:

(1) The wind profile within the PBL differs distinctly from that described by the

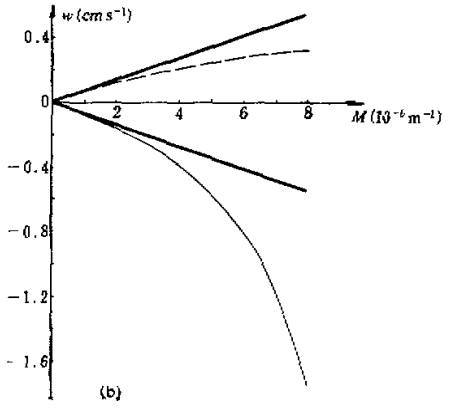

Fig. 2b. Same as Fig. 2a, except for neutral condition.

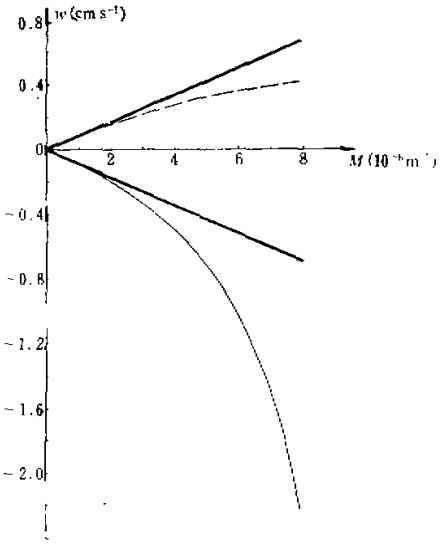

Fig. 2c. Same as Fig. 2a, except for unstable condition.

classical Ekman spiral when one takes account of the nonlinear advection effect. The distinction between the wind distributions depends upon the pressure system. With employing the geostrophic momentum approximation, the nonlinear advection accelerates the air to move in the high pressure area and decelerates in the low pressure area. This conclusion conforms to the results of Ref. [2].

(2) The stratification and surface roughness length have certain influence on the wind profile in the lower Ekman layer.

(3) The correction of the nonlinear advection effect to the vertical velocity at the top of the PBL includes factors such as surface roughness and stratification besides geostrophic vorticity.

(4) The atmospheric baroclinity plays an important role in altering the wind distribution within the Ekman boundary layer.

In this paper, based on the geostrophic momentum approximation, the linear and nonlinear Ekman solutions incorporating baroclinity are derived by matching the Ekman layer with the surface layer, so that they can be widely used. In fact, the proposed theory has been applied successfully to the numerical diagnostic analysis of the surface wind over the sea. This work will be published in another paper.

REFERENCES

[1] Wu Rongsheng and Blumen, W. (1982), An analysis of Ekman boundary layer dynamics incorporating the geostrophic momentum approximation, *J. Atmos. Sci.*, **39**: 1774—1782.

[2] Wu Rongsheng (1984), Dynamics of non-linear Ekman boundary layer, *Acta Meteorologica Sinica*, **42**: 269—278 (in Chinese with English abstract).

[3] Businger, J., Wyngaard, J. C., Izumi, Y. and Bradley, E. (1971), Flux profile relationships in the atmospheric surface layer. *J. Atmos. Sci.*, **28**: 1021—1025.

[4] Cherney, J. G. and Eliassen, A. (1949), A numerical method for predicting the perturbations on the middle latitude westerlies, *Tellus*, **1**: 38—54.